

## *Events of enhanced convection and related dayside auroral activity*

Article

Published Version

Moen, J., Sandholt, P. E., Lockwood, M. ORCID: <https://orcid.org/0000-0002-7397-2172>, Denig, W. F., Løvhaug, U. P., Lybekk, B., Egeland, A., Opsvik, D. and Friis-Christensen, E. (1995) Events of enhanced convection and related dayside auroral activity. *Journal of Geophysical Research*, 100 (A12). p. 23917. ISSN 0148-0227 doi: 10.1029/95JA02585 Available at <https://centaur.reading.ac.uk/38796/>

It is advisable to refer to the publisher's version if you intend to cite from the work. See [Guidance on citing](#).

Published version at: <http://dx.doi.org/10.1029/95JA02585>

To link to this article DOI: <http://dx.doi.org/10.1029/95JA02585>

All outputs in CentAUR are protected by Intellectual Property Rights law, including copyright law. Copyright and IPR is retained by the creators or other copyright holders. Terms and conditions for use of this material are defined in the [End User Agreement](#).

[www.reading.ac.uk/centaur](http://www.reading.ac.uk/centaur)

**CentAUR**

Central Archive at the University of Reading

Reading's research outputs online

## Events of enhanced convection and related dayside auroral activity

J. Moen,<sup>1</sup> P. E. Sandholt,<sup>2</sup> M. Lockwood,<sup>3</sup> W. F. Denig,<sup>4</sup> U. P. Løvhaug,<sup>5</sup>  
B. Lybekk,<sup>2</sup> A. Egeland,<sup>2</sup> D. Opsvik,<sup>2</sup> and E. Friis-Christensen<sup>6</sup>

**Abstract.** In this paper we study the high-latitude plasma flow variations associated with a periodic (~8 min) sequence of auroral forms moving along the polar cap boundary, which appear to be the most regularly occurring dayside auroral phenomenon under conditions of southward directed interplanetary magnetic field. Satellite data on auroral particle precipitation and ionospheric plasma drifts from DMSP F10 and F11 are combined with ground-based optical and ion flow measurements for January 7, 1992. Ionospheric flow measurements of 10-s resolution over the range of invariant latitudes from 71° to 76° were obtained by operating both the European incoherent scatter (EISCAT) UHF and VHF radars simultaneously. The optical site (Ny Ålesund, Svalbard) and the EISCAT radar field of view were located in the postnoon sector during the actual observations. The West Greenland magnetometers provided information about temporal variations of high-latitude convection in the prenoon sector. Satellite observations of polar cap convection in the northern and southern hemispheres show a standard two-cell pattern consistent with a prevailing negative  $B_y$  component of the interplanetary magnetic field. The 630.0 nm auroral forms located poleward of the persistent cleft aurora and the flow reversal boundary in the ~1440–1540 MLT sector were observed to coincide with magnetosheath-like particle precipitation and a secondary population of higher energy ions, and they propagated eastward/tailward at speeds comparable with the convection velocity. It is shown that these optical events were accompanied by bursts of sunward (return) flow at lower latitudes in both the morning and the afternoon sectors, consistent with a modulation of Dungey cell convection. The background level of convection was low in this case ( $K_p=2^+$ ). The variability of the high-latitude convection may be explained as resulting from time-varying reconnection at the magnetopause. In that case this study indicates that time variations of the reconnection rate effectively modulates ionospheric convection.

### 1. Introduction

Observations during the last 2–3 decades have demonstrated that magnetospheric convection and the associated ionospheric plasma flow are strongly controlled by the orientation of the solar wind magnetic field [e.g., Cowley, 1982; Reiff and Burch, 1985; Lockwood and Freeman, 1989; Rich and Hairston, 1994, and references therein]. *Etemadi et al.* [1988] and *Todd et al.* [1988] found by combining European incoherent scatter (EISCAT) UHF ion drift measurements and AMPTE observations of the interplanetary magnetic field (IMF) that the dayside convection

responds rapidly to southward swings of the IMF. However, the nature of the solar wind-magnetospheric coupling, i.e., the mechanisms within the magnetospheric boundary layers (earthward of the magnetopause) by which energy and momentum are transferred from the solar wind to the high-latitude magnetosphere-ionosphere convection, are far from being fully understood. One way to improve our understanding on this point is to study cusp/cleft ionospheric activity by different techniques. This paper is devoted to the ongoing debate concerning the impact boundary layer processes related to cusp/cleft auroral activity have on polar cap convection. *Lockwood et al.* [1989] and *Pinnock et al.* [1993] presented EISCAT and PACE HF radar observations, respectively, of bursty ionospheric plasma flow being attributed to enhancements of the magnetic reconnection rate. *Lockwood et al.* [1990a] argued that transitory magnetic reconnection may contribute a considerable fraction to the cross-polar potential drop. *Denig et al.* [1993] concluded, based on their case study, that transient magnetic reconnection events (FTEs) may give only minor supply to the global-scale convection pattern. They argued from the observed north-south voltage (associated with longitudinal flow) across the events. *Lockwood and Cowley* [1994] pointed out that this voltage may depend on IMF  $B_y$  and that

<sup>1</sup> University Courses on Svalbard, Longyearbyen, Norway.

<sup>2</sup> Department of Physics, University of Oslo, Norway.

<sup>3</sup> Rutherford Appleton Laboratory, Chilton, Didcot, England.

<sup>4</sup> Geophysics Directorate, PL/GPSG, Hanscom Air Force Base, Massachusetts.

<sup>5</sup> EISCAT Scientific Association, Ramfjordmoen, Norway.

<sup>6</sup> Division of Geophysics, Danish Meteorological Institute, Lyngbyvej, Copenhagen, Denmark.

the most relevant voltage associated with the dayside auroral events is the flux addition rate which may be large.

A most common category of cusp/cleft auroral transients, described in detail by *Sandholt et al.* [1986, 1989, 1993a, b], occur predominantly during periods of southward directed IMF as a series of auroral forms moving along the polar cap boundary and into the polar cap. This event category has tentatively been related to transient magnetic reconnection at the dayside magnetopause [*Russell and Elphic*, 1979] for several reasons, including their similar occurrence rates and dependencies on the IMF orientation. Each event signature initially appears as a localized intensification of the cusp/cleft aurora. This brightening structure propagates in the east-west direction (controlled by the IMF  $B_y$  component) and separates from the background arc on the poleward side, forming an auroral form there. The initial motion of this form is consistent with the effect of magnetic tension on newly merged flux [e.g., *Cowley et al.*, 1991]. After ~10 min, the auroral form fades on mantle field lines [*Sandholt et al.*, 1993b]. The event recurrence period is 8 min on average. *Lockwood et al.* [1989] related this category of optical transients to flow bursts in the EISCAT radar data when IMF  $|B_y|$  was large. The onset of enhanced convection speed was observed to precede each fast-moving auroral form. Observations by *Sandholt et al.* [1993a, b] indicated that the auroral forms of this category broadly follow the average streamlines of the empirical *Heppner and Maynard* [1987] convection patterns for the measured IMF conditions.

Several models of ionospheric flow signatures associated with FTEs have been proposed. A frequently used description of FTE flow excitation is the "moving cloud-model" equivalent to the flow around a cylinder of circular or elliptical cross section moving in the ambient ionospheric plasma [*Southwood*, 1987; *Lockwood et al.*, 1990b; *Wei and Lee*, 1990]. The principal idea behind such models is that the flow inside the flux rope is uniform and that the surrounding ionospheric plasma (incompressible) is set into a twin-vortical motion as the path of the faster moving flux tube is pushed out. *Wei and Lee* [1990] pointed out that an elongated plasma cloud and hence a twin-vortex convection pattern may originate from an impulsive plasma penetration event (PTE) as well. The auroral footprint corresponding to a plasma cloud penetrating the LLBL must move from the open/closed field line boundary to closed field lines and hence is expected to have an equatorward rather than a poleward motion component relative to the background arc [*Goertz et al.*, 1985; *Heikkila et al.*, 1989]. Filamentary plasma injections into the plasma mantle are also feasible. The auroral footprint associated with such events are expected to remain at the poleward side of the cleft arc. For any mantle event of the PTE-class, the azimuthal component of motion is expected to be tailward away from noon independent of the IMF  $B_y$  polarity. Thus the appearance and motion of the auroral transients relative to the preexisting background arc may be an important discriminating criterion for distinguishing between PTEs and FTEs [cf. *Goertz et al.*, 1985; *Sandholt et al.*, 1993a].

*Friis-Christensen et al.* [1988] and *Sibeck* [1990] proposed that dynamic pressure variations at the magnetopause may create traveling convection vortices (TCVs) in the ionosphere-magnetosphere system [cf. *Glassmeier*, 1992]. *Kivelson and Southwood* [1990] argued that a single pres-

sure pulse creates a pair of oppositely rotating vortices associated with a pair of oppositely directed Birkeland currents. *McHenry et al.* [1990a, b] identified a continuous series of TCVs located near the convection reversal boundary on field lines mapping to the inner edge of low-latitude boundary layer (LLBL) and suggested that these vortices are signatures of the Kelvin-Helmholtz instability. The whole sequence of east-west chain of vortices was found to be moving generally antisunward and neighboring vortices to have opposite rotation direction. Pressure pulse and Kelvin-Helmholtz generated vortices propagate along the line combining the Birkeland current pair, while the FTE and PTE flow vortices move perpendicular to this line, and may be distinguished from each other by high-resolution convection measurements.

*Cowley and Lockwood* [1992] proposed a model for large-scale flow excitation due to FTEs based on the concept of zero-flow equilibrium configurations of the magnetosphere which have an arbitrary amount of open flux, a work inspired by the theoretical convection-model of *Siscoe and Huang* [1985] and the explanation of ionospheric effects of magnetospheric erosion by *Freeman and Southwood* [1988] [cf. *Lockwood et al.*, 1990a]. During southward IMF conditions the effect of impulsive magnetopause reconnection is to increase the amount of open flux in the magnetosphere. A two-cell convection pattern (strongest in the dayside ionosphere) is then excited to move the system back towards a new equilibrium situation, in which the polar cap has expanded. Conversely, for tail reconnection, a distortion from equilibrium configuration occurs as an amount of open flux is destroyed. Again, a two-cell convection pattern (greatest in the nightside ionosphere) is excited to achieve a new equilibrium situation where the polar cap has become smaller. The IMF  $B_y$  related asymmetry of flow cells is expected to be as for continuous reconnection. In contrast to the *Southwood* [1987] model where an FTE footprint creates a moving small-scale flow distortion of minor importance for the large-scale polar cap convection, the *Cowley and Lockwood* [1992] model propose that each FTE will subsequently influence the entire polar cap convection pattern.

In this paper, horizontal plasma flow measured by the EISCAT UHF and VHF radars is combined with simultaneous ground based optical recordings from Ny Ålesund, Svalbard (78.9° N, 11.9° E). A sequence of ionospheric transients in the postnoon sector on January 7, 1992, is investigated. The ionospheric transients belong to an extended sequence of auroral activity following a sharp activity onset at 1033 UT. *Lockwood et al.* [1993a] interpreted this activity onset as being a consequence of southward turning of the IMF. The poleward limit of the combined EISCAT UHF/VHF field of view was roughly at the ionospheric flow reversal boundary, which is also the latitude of the optical site. Transient events of sunward flow were detected by the radars. A corresponding sequence of eastward moving auroral forms were observed poleward of the radar field of view. The objective of the current paper is to study different aspects of the excitation of flow associated with the transient auroral activity; i.e., particle precipitation characteristics, boundary motions, and field-aligned currents. A comparison of direct flow measurements in the postnoon sector and indirect flow information obtained from Green-

land magnetometers in the prenoon sector indicates that the auroral forms were associated with the modulation of large-scale high-latitude convection.

The following section briefly describes the instrumentation techniques employed in this study which include a multichannel meridian scanning photometer (MSP) and an all-sky TV camera in Ny-Ålesund, the EISCAT UHF and VHF radars, the particle experiment and plasma flow instruments on board the DMSP satellites, and the chain of ground magnetometers at the west coast of Greenland. We then show examples of moving auroral forms accompanied by convection enhancements. In the discussion section the event characteristics are compared with the ionospheric signatures expected of the different boundary layer mechanisms discussed above. Two different models of FTE flow excitation are emphasized, i.e., the *Southwood* [1987] and the *Cowley and Lockwood* [1992] models. Finally, a brief summary is given.

## 2. Instrumentation

The optical instrumentation at Ny Ålesund (76° ILAT) includes a four-channel meridian scanning photometer (MSP) and a charged-coupled-device (CCD) television camera. The TV camera is filtered at 630.0 nm to observe auroral red line emissions. The MSP has a 2° field of view and scans along the magnetic meridian to  $\pm 80^\circ$  from zenith. The MSP scan period is 18 s. The four-filter MSP has channels sensitive to the 630.0 nm and 557.7 nm atomic oxygen (O I) emissions, the first  $N_2^+$  negative band transition at 427.8 nm, and the hydrogen  $H_\beta$  line at 636.5 nm. In the present study only the red and green O I lines will be

considered. These correspond to transitions from the metastable states,  $^1D$  and  $^1S$  respectively, of atomic oxygen. Atomic oxygen in the  $^1S$  state returns to the ground state ( $^3P$ ) via the intermediate level  $^1D$ . The average lifetimes of the  $^1S$  and  $^1D$  states are 0.7 and 110 s, respectively. The long lifetime of the O I  $^1D$  state results in collisional quenching at low altitudes and a red line peak emission in the *F* region, while the green line emission intensity peaks at lower altitudes in the *E* region.

The EISCAT UHF and VHF radars were operated simultaneously in the SP-UK-CONV experiment mode appropriate for plasma flow measurements above the Svalbard region. In this particular mode, the UHF radar points 16° west of geographical north at an elevation angle of 20°. The VHF radar is operated at its minimum elevation of 30° pointing in a direction 15° to the east of the UHF beam (cf. Figure 1). Assuming the ion flow to be constant along the *L* shell over the distance between the beams (increasing from 110 km at 71° ILAT to 220 km at 76° ILAT), 10-s resolution horizontal plasma flow vectors are obtained by combining line-of-sight velocities from the two radars. Note that these vectors must be treated with caution because of the *L* shell assumption. Ion flow vectors are derived at 17 adjacent gates ( $\sim 35$  km) covering the range of invariant latitudes 71°–76°. Figure 1 also shows the optical field of view, relative to the EISCAT UHF and VHF radar beams. The straight line through Ny Ålesund demonstrates the latitudinal survey of the MSP scan, assuming a peak emission altitude of 300 km. The circle demonstrates the useful field of view of the all-sky 630.0 nm TV camera.

Complementary information about auroral particle precipitation and ionospheric plasma flow is provided by the sun-synchronous, polar orbiting DMSP F10 and F11 satellites. These satellites, which are in circular orbits at about 850 km, are instrumented with separate electron and ion ElectroStatic Analyzers (ESA) having fields of view along the local zenith. The ESA measure the energy spectrum, once per second, of precipitating charged particles within the range from 32 eV to 32 keV. Each satellite is also equipped with a thermal plasma drift meter (DM) and a retarding-potential analyzer (RPA). The DM measured the horizontal and vertical cross-track velocity components of the ionospheric plasma, while the RPA measured the plasma flow component along the orbital trajectory. The F10 data used in this study were acquired during the pass as indicated in Figure 1 by the straight line, nearly normal to the photometer scanning plane, and crossing the Svalbard meridian at 1152 UT on this day. The northern-southern hemisphere dawn-dusk passes of the F11 satellite during the 1000–1230 UT interval were used to deduce large-scale convection patterns and probable IMF conditions.

Ground-magnetometer observations from the Greenland west coast stations provided indirect information about the time variations of the polar cap convection. This chain of magnetometers consists of 10 stations covering the range of invariant latitudes from 66.9° to 85.7° ILAT, with magnetic local noon at  $\sim 1400$  UT. (This should be compared with 12 MLT = 0850 UT for the Ny Ålesund site; i.e., the Greenland sites are roughly at an MLT 5 hours earlier than that at Ny Ålesund.) In this paper we will be considering data collected during the time interval 1130–1230 UT on January 7, 1992. During this time period, Ny Ålesund was in the magnetic postnoon sector ( $\sim 1440$ – $1540$  MLT) while the Greenland

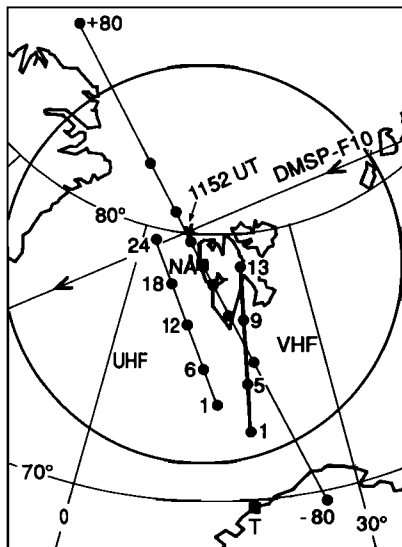


**Figure 1.** Map showing the EISCAT UHF and VHF radar beams employed by the SP-UK-CONV experiment. The numbered dots mark the range gate centers. The straight line through Ny Ålesund (NÅ) shows the meridian scanned by the 630.0 nm photometer, onto which dots indicate the locations of 20° steps in zenith angle assuming an emission altitude of 300 km. The circle with its center at Ny Ålesund roughly indicates the useful field of view of the all sky 630.0 nm TV camera. Also shown is the DMSP-F10 pass intercepting the scanning meridian by 1152 UT.

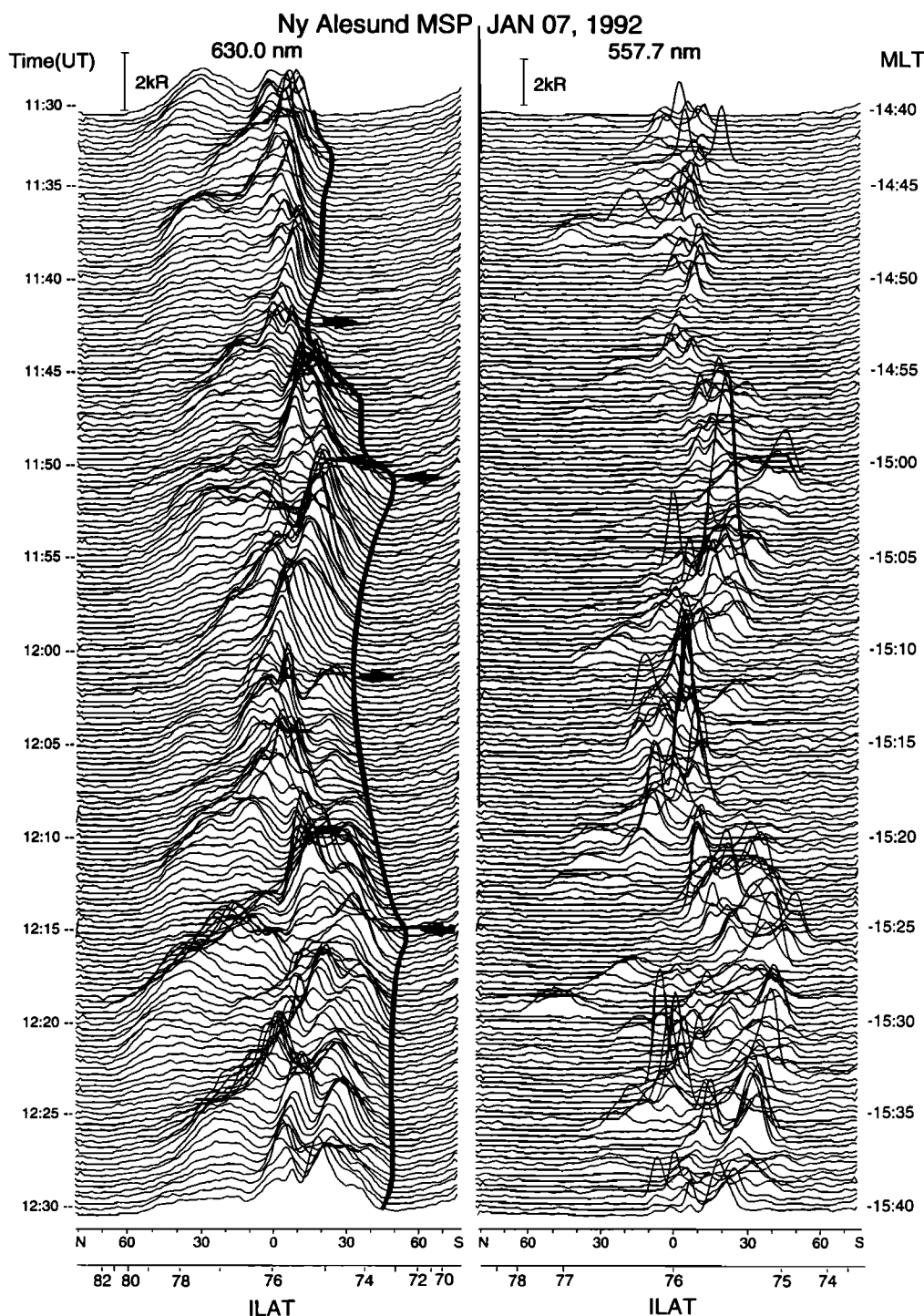


**Figure 2.** Magnetic north (N) - south (S) meridian photometer scans at wavelength (left) 630.0 nm and (right) 557.7 nm obtained at Ny Ålesund during the time interval 1130-1230 UT (1440-1540 MLT) on January 7, 1992. The ILAT scales correspond to altitudes of red and green line O I emissions of 300 km and 120 km, respectively. The auroral transients appear as intermittent 630.0 nm intensifications at the poleward side of the more continuous background arc which was a mixture of red and green line emissions. The solid line marks the equatorward border of the 630.0 nm emission, and the arrows mark the onsets of north-south motions of this boundary.

west coast was in the prenoon sector. The magnetic local time extension of the instrumentation is essential for the identification of the spatial extent of the energy and momentum transfer associated with the auroral events and its influence on large-scale polar cap convection.

### 3. Observations

#### 3.1. Optical Data From Ny Ålesund

Figure 2 shows stacked photometer traces at wavelengths 630.0 nm and 557.7 nm acquired during a 1-hour interval from 1130 to 1230 UT (1440-1540 MLT) on January 7,

1992. Each trace represents the zenith angle distribution of line-of-sight intensity along the north (N) - south (S) scan. The nonlinear scales of invariant latitudes corresponding to zenith angle position of the photometer were obtained by assuming peak altitudes of 120 km and 300 km for the red- and green-line emissions, respectively. A quasi-periodic sequence of auroral transients occurred poleward of a semipersistent background luminosity, i.e., between zenith and  $45^\circ$  to the north. During the 2 hours period from 1130 to 1330 UT, 14 such auroral events occurred, giving an average recurrence period of  $\sim 8$  min. As regards to the spectral composition, these transient forms are strikingly different from the aurora south of zenith. While the former auroral brightenings were red-dominated, strong, but highly variable 557.7 nm intensities ( $\sim 5$  kR) were recorded within the background emission. All-sky TV imagery shows that the sequence of red-line enhancements seen by the MSP was associated with a series of intermittent auroral forms that drifted through the scanning meridian from west to east. These auroral forms formed outside the circular area of optical coverage, likely somewhere above Greenland, closer to magnetic noon. Some 5-10 min after the events arrived the TV field of view, they faded out just poleward of the background arc. This occurred near the Ny Ålesund meridian or, for the longer-lived events, slightly to the east of it. Plate 1 presents a sequence of digitized all-sky TV images at 1-min intervals. This particular image sequence (for the interval 1212 to 1223 UT) was chosen to demonstrate the temporal and spatial evolution of that event which entered the scanning meridian about 1217 UT (cf. Figure 2). Each of the 12 images represents an average of 1.28 s video-recording, starting at the time indicated on each frame. The all-sky display has been transformed to geographic coordinates assuming an  $F$  region emission height of 300 km. The images are limited by the  $70^\circ$  zenith angle circle, outside which the camera sensitivity falls rapidly. From 1212 UT onward, an auroral form propagated into the camera field of view. Around 1217 UT, the eastern point of this east-west elongated arc segment touched the poleward boundary of the background arc close to Ny Ålesund. This point acted as a pivot around which the elongated auroral form started rotating. The auroral form rotated through  $\sim 180^\circ$  rotation before it faded out, to the east of the Ny Ålesund meridian. The all-sky imagery of the other 14 events between 1130 to 1330 UT has been examined in detail. Most of them propagated eastward on the poleward side of the background arc without showing such a prominent rotation as demonstrated in Plate 1. There was a clear tendency for only the most east-west extended optical events to rotate. When looking at such all-sky camera displays, one must be aware that artificial effects may be introduced by projection to a certain altitude of a height distribution of the auroral emission. For example, by this projection technique an east-west elongated rayed arc structure may appear as a fan-shaped form. If such an arc feature moves in east-west direction an artificial rotation may result. Without information about the energy spectra of the incoming electrons, or about the height distribution of the emissions, it cannot be guaranteed that the rotation seen in Plate 1 was a real rotation or not. However, this is quite uncritical for the conclusions made in this paper. What is important, however, is that all the events had a strong eastward component of motion.

### 3.2. F10 Svalbard Overpass

A digitized TV image taken at 1154 UT mapped onto a geographical reference frame is presented in Figure 3 for comparison with direct auroral particle measurements provided by an F10 overflight near Svalbard at 1152 UT. This comparison therefore allows for the mean radiative lifetime of  $D$  state of 110 s between excitation and emission of the 630.0 nm photon. An auroral transient that was propagating eastward is seen poleward of the band of background luminosity. The white line running from east to west poleward of Svalbard marks the satellite trajectory projected along the magnetic field down to an altitude of 300 km. Plate 2a shows the electron and ion precipitation fluxes versus energy and time, respectively. From 1151.30 to 1154.30 UT F10 traversed a region of strongly enhanced fluxes of low-energy electrons ( $< 400$  eV) and ions ( $< 1$  keV), i.e., magnetosheath-like plasma which has not been much accelerated during the entry process [Newell and Meng, 1988]. Let us consider the electron precipitation in particular which is assumed to be the source of auroral emissions. From 1151.30 to 1152 UT, the electron flux rapidly increased. Viewing along the satellite track in Figure 3 for this time interval we can imagine a corresponding increase in the red line emission intensity. It should be remembered that the camera sensitivity is falling away from zenith.

Plate 2b shows the F10 along-track component of ion drift obtained from the retarding potential analyzer (RPA). A positive (negative) sign of the along-track component refers to plasma flow antiparallel (parallel) to the direction of satellite motion. For example, at the time when the satellite intercepted the region of magnetosheath-like plasma precipitation/optical event, a strong eastward component ( $\sim 1.5$  km  $s^{-1}$ ) of flow was measured. This agrees very closely with the east-west motion of the auroral event, as inferred from all-sky TV video recordings. The observed eastward flow began with a rapid change of the ion flow direction at 1148.40 UT indicating a flow reversal at ( $\sim 73^\circ$  MLAT;  $\sim 17.6$  MLT).

From 1151 to 1154 UT F10 was almost tracking the  $L$  shell on the way towards magnetic noon (from  $\sim 15$  MLT to  $\sim 13.25$  MLT). From then on the satellite moved to lower  $L$  values. In this region of sheath-like precipitation, the satellite observed an ascending (with time) ion dispersion signature. From 1151.50 to 1154 UT, the ion energy spectrum seems to be spatially separated in three regions of enhanced ion flux (centered at  $\sim 1152$ , 1152.50, 1153.40 UT), presumably related to a succession of three events. The optical event in Figure 3 is associated with the first one of these precipitation regions, as it took the satellite about 1 min to cross through this auroral form. With an average convection speed of  $1.5$  km  $s^{-1}$  it is estimated to take roughly 5 min for the second precipitation event to reach the scanning-meridian. As seen from Figure 2, the 1152 UT event was actually followed by another event  $\sim 5$  min later. The third precipitation region crossed by the satellite was however not observed to reach the optical field of view. (The all-sky TV video recordings have been checked.)

Figure 4 shows six pairs of 10-s averaged electron and ion spectra covering the 1 min time interval 1152 to 1153 UT. In addition to the strong flux of magnetosheath-like ions, a secondary population of higher-energy ions (1-30 keV) forming a shoulder is apparent in some of the profiles.

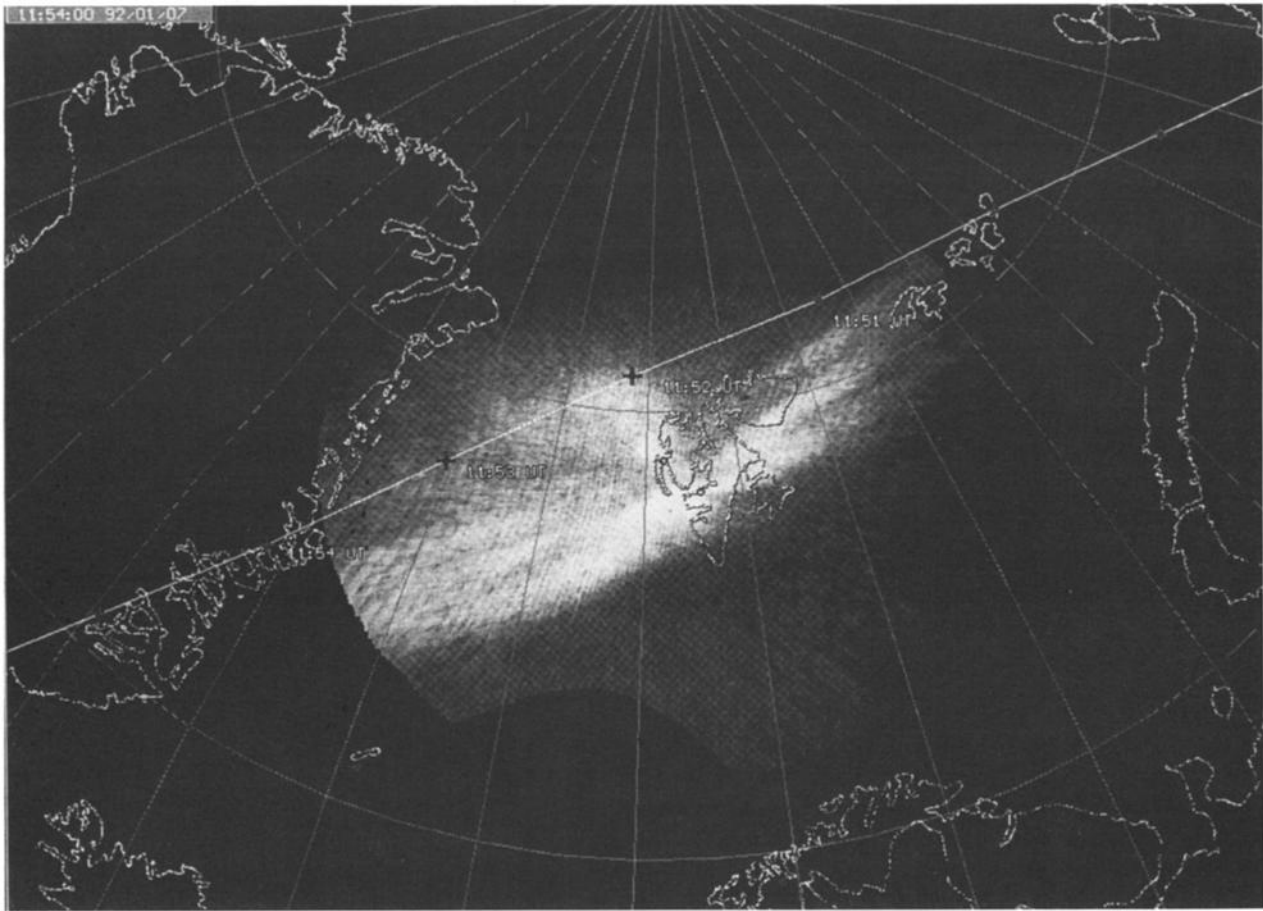


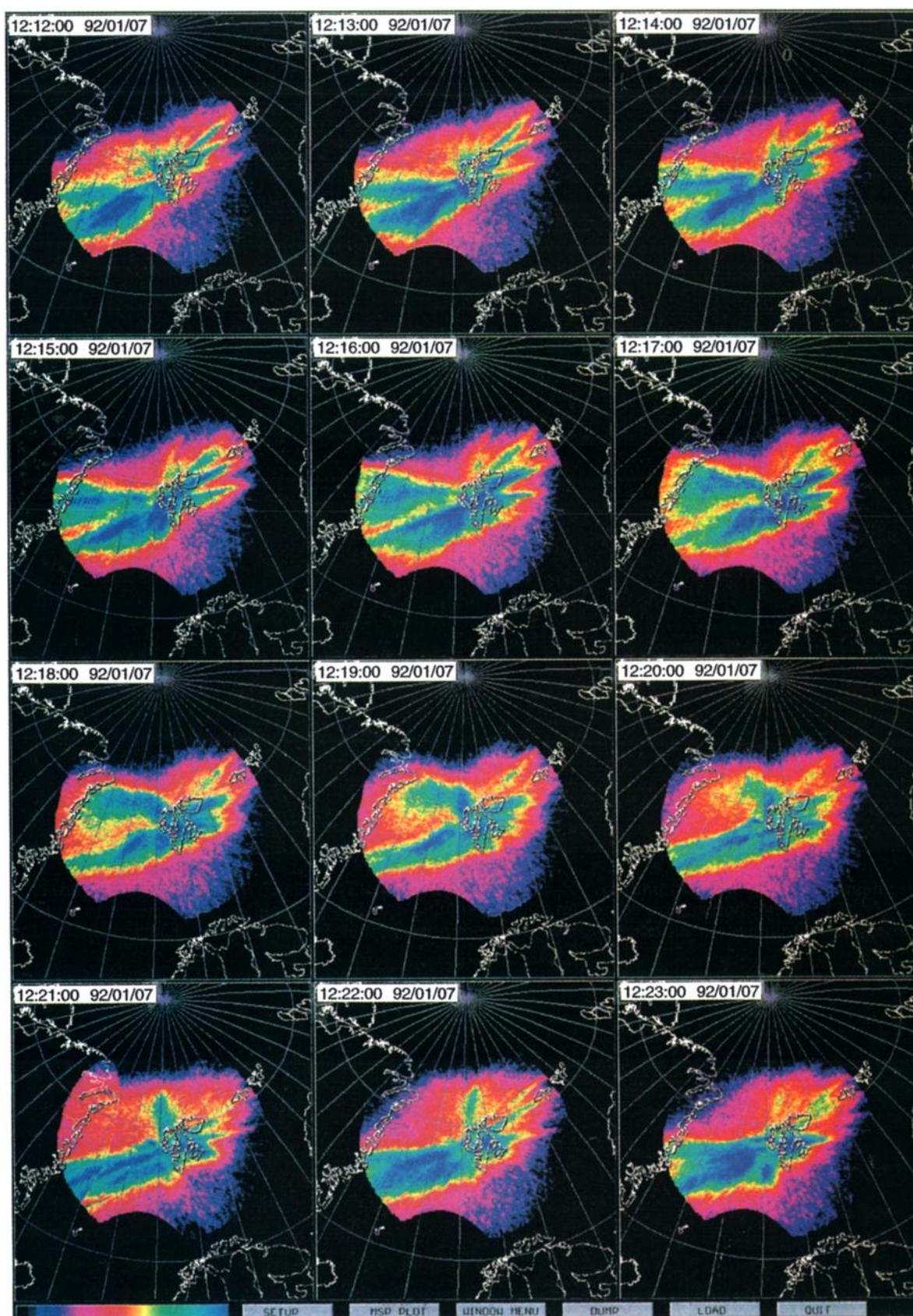
**Figure 3.** A digitized all-sky camera image taken at 1154 UT mapped onto a geographical frame of reference. The F10 satellite pass is indicated by the white line, onto which the satellite coordinates at 1151, 1152, 1153, and 1154 UT are marked by crosses. Allowing for the O I  $^1D$  excitation state lifetime of 110 s the auroral picture is best corresponding to the F10 particle measurements near 1152 UT.

### 3.3. EISCAT Convection Measurements in Relation to Aurora

Plates 3a and 3b show the line-of-sight velocity ( $v_{los}$ ) measured by the EISCAT UHF radar as function of time and invariant latitude for the intervals 1130–1200 UT (1440–1510 MLT) and 1200–1230 UT (1510–1540), respectively. Because the UHF radar points nearly along the magnetic meridian at low elevations, this line-of-sight velocity is, to a good approximation, equal to the northward convection velocity component. In order to enhance the characteristic features of velocity variations, slightly different speed ranges have been chosen on the color bars on these two plots. However, they are both ranging from blue to red in order of increasing velocity from negative to positive values. Negative  $v_{los}$  means southward moving plasma (towards the radar site near Tromsø), and positive  $v_{los}$  is poleward moving plasma (away from the radar). Major variations in the line-of-sight velocity were observed between 75° and 78° ILAT. During the one hour interval from 1130 to 1230 UT, the sign of  $v_{los}$  alternated four times. This motion pattern can be compared with the observed latitudinal motions of the background aurora. The heavy line in Figure 2 marks the equatorward boundary of the 630.0 nm emissions. The arrows mark the onsets of directional changes of this

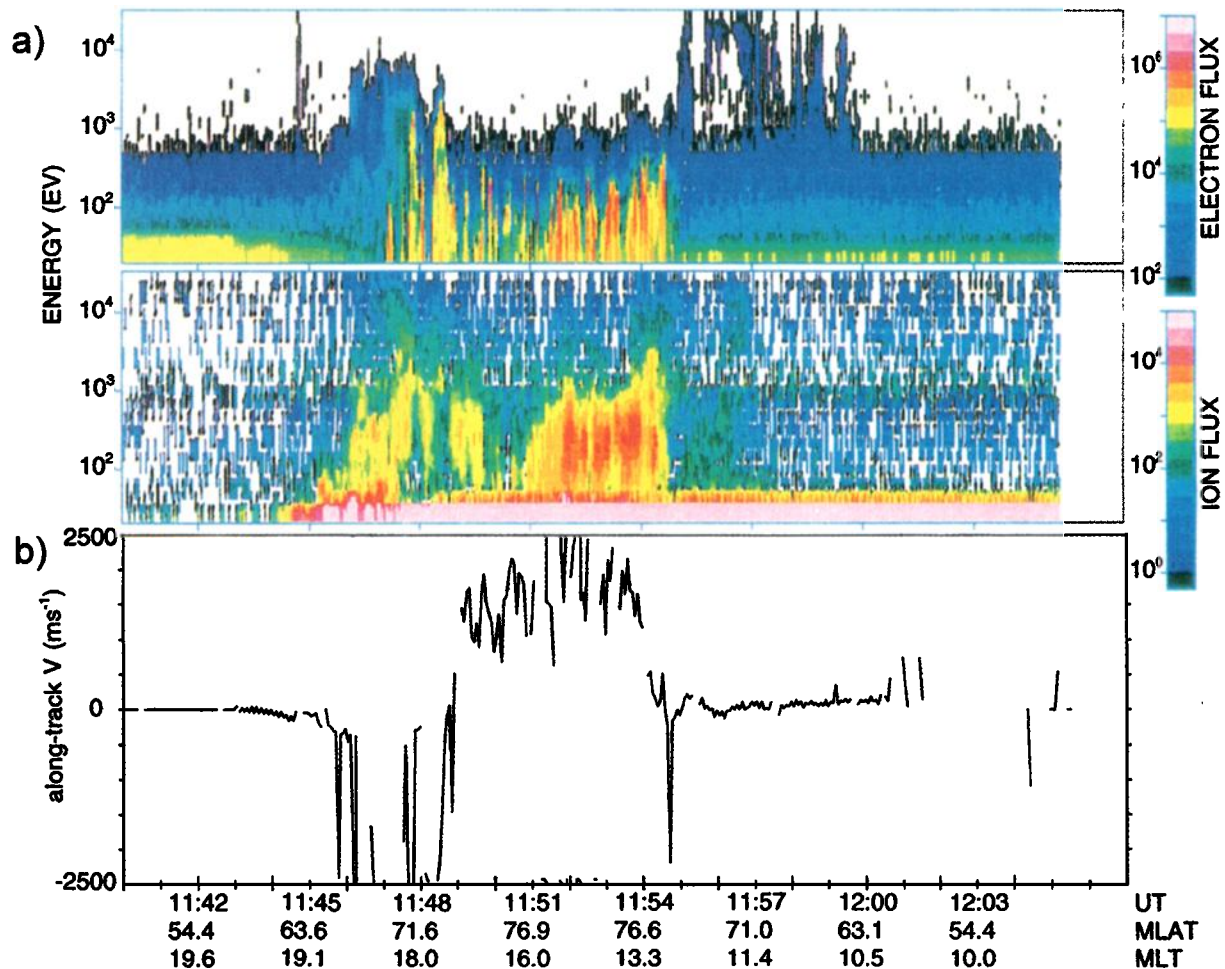
boundary motion. During the time intervals 1133–1143 UT, 1151–1201 UT, and 1215–1230 UT the southern 630.0 nm boundary moved poleward, and during the intervals 1143–1151 UT and 1201–1215 UT this boundary moved equatorward. It is clear that the intervals of alternating north-south auroral motions coincide with corresponding changes in the direction of the line-of-sight plasma velocity. For the assumed emission altitude of 300 km, the arc boundary moves with similar speed as the ionospheric plasma. For example from 1151 to 1201 UT it moved poleward from 73.1° to 74.4° ILAT with an average velocity of 240 m s<sup>-1</sup>, which is comparable to the observed EISCAT line-of-sight velocities at the same latitudes. The period of latitudinal motions of the southern 630.0 nm arc border, is 15 min on the average, about twice the intermediate time between successive events. From the EISCAT data in Plate 3a and 3b the plasma motions at higher latitudes appear to be considerably larger.

Figure 5 shows the 10-s resolution ion flow vectors obtained from the SP-UK-CONV experiment as function of invariant latitude and time. The common EISCAT UHF and VHF radars field of view covered invariant latitudes from 71° to 76°. The moving auroral forms were detected poleward of Ny Ålesund and hence poleward of this field of



**Plate 1.** Digitized all-sky 630.0 nm TV camera images from Ny Ålesund mapped onto a geographical frame of reference (for an assumed emission altitude of 300 km) for the time period interval 1212-1223 UT. The dynamic synthetic color scale was set to the most intense auroral feature within the sequence.

## DMSP F10 JAN. 07, 1992



**Plate 2.** (a) F10 auroral particle energy-time spectrograms for the pass slightly poleward of the Svalbard region around 1152 UT on January 7, 1993. Electron and ion spectra are given in the upper and the lower panel, respectively. The auroral particle fluxes measured from 1151.50 UT onward correspond to the transient auroral event seen poleward of background arc in Figure 3. (b) Along-track component of plasma flow during the Svalbard overpass of F10 at 1152 UT on January 7, 1992.

view. The major sunward (westward) convection enhancement within 1213–1221 UT shown in Figure 5, occurred equatorward of the auroral form presented in Plate 1. The flow vectors reveal a relatively steady northwestward flow direction. The channel of enhanced convection was located within the belt of background luminosity. The correlation between enhancements in the ionospheric convection and the auroral activity will be demonstrated in section 4.4.

### 3.4. F11 Measurements of Global Scale Convection

Figure 6 presents plots of the cross-track ion drifts acquired by F11 during four successive northern and southern hemisphere passes on January 7, 1992. The data are plotted on a MLAT/MLT polar dial, where dawn (0600 MLT) is to the right and local noon (1200 MLT) is at the top of each diagram. The outer circle represents the 50° MLAT circle, and the dotted circles mark 60°, 70° and 80° MLAT. The time (UT) refer to the maximum magnetic latitude (MLAT) of each pass.

The first northern high-latitude pass at 0957 UT revealed

weak convection in the polar cap and hence extremely quiet conditions. Comparing this pass with the following southern dawn-to-dusk crossing at 1050 UT, a major flow enhancement must have taken place during the interval between these passes. The high-latitude convection observed during the 1050 and 1229 UT southern passes resembles *Heppner and Maynard* [1987] type BC convection, whereas the 1139 UT northern pass corresponds to their type DE convection pattern. Characteristically, in the northern (southern) hemisphere the evening (morning) cell convection reversal took place over a narrow latitudinal region as expected within a crescent-shaped cell. These convection patterns, with a large (small) dawn-cell and small (large) dusk-cell in the northern (southern) hemisphere, are characteristic of prevailing negative IMF  $B_y$  [Freeman *et al.*, 1993].

### 3.5. Magnetometer Data From the Greenland West Coast

Figure 7 shows the  $H$  component magnetometer recordings from stations on Greenland west coast recorded during the interval 1000–1400 UT on January 7, 1992. The station

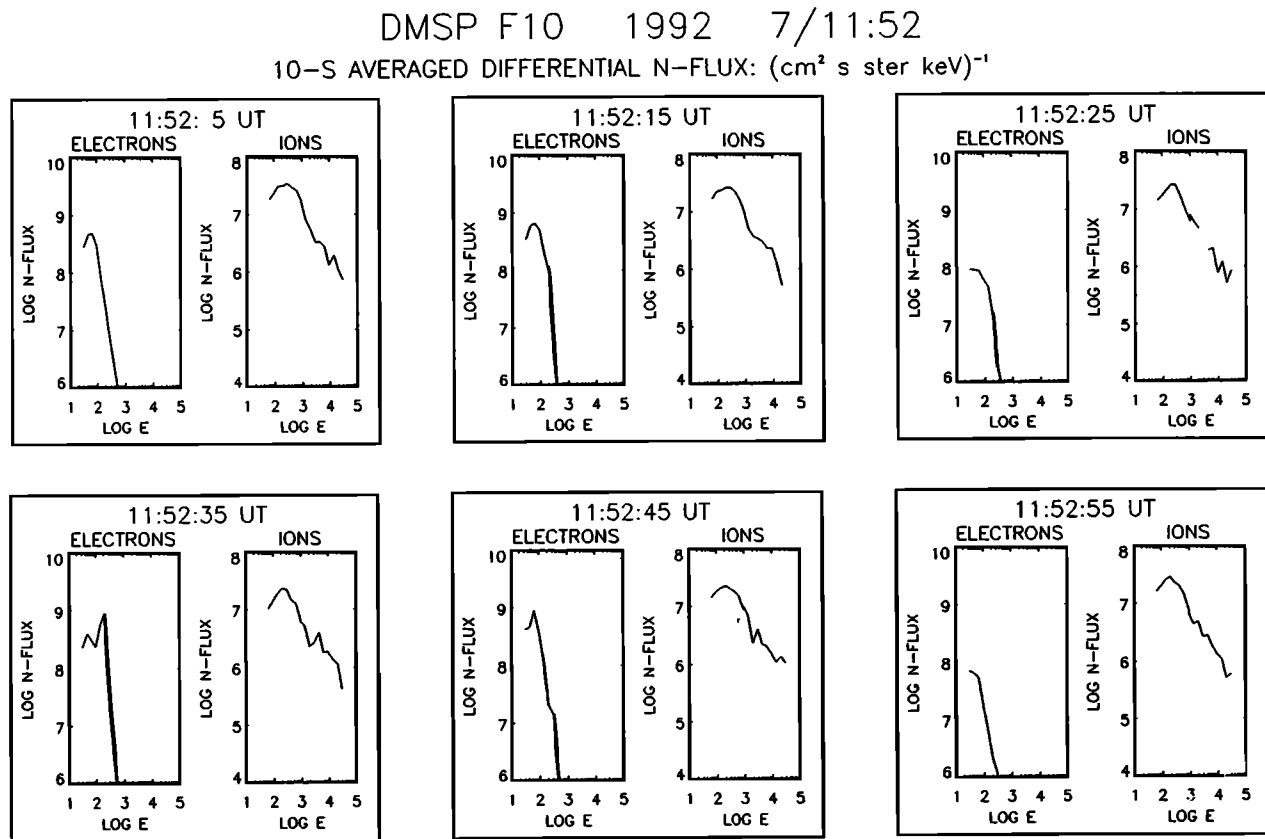


**Figure 4.** Full profile electron and ion energy spectra taken by DMSP F10 when crossing through the auroral form as shown in Figure 3.

codes and latitudinal positions are given respectively on the left- and right-hand sides of the stacked magnetograms. Thule (THL) is the northernmost and Narssarsuaq (NAQ) the southernmost station. After about 1030 UT, the  $H$  component at all the stations from 72.5° to 85.7° ILAT exhibited a negative excursion that lasted about 2 hours. Correspondingly, the  $E$  component (eastward; not shown) revealed a positive deflection. This is consistent with a southwestward directed Hall current associated with a northeastward ionospheric plasma convection. The latitudinal location of the westward Hall current can be determined by the change in  $Z$  component polarity (not shown), from positive to negative, when going toward lower latitudes. Thus, during the 1130–1230 UT interval, the center of the Hall current distribution and hence the strongest convection was located between ATU (75° ILAT) and GDH (76.2° ILAT). The present study of plasma flow variations in relation to auroral activity focuses on the time window from 1145 to 1230 UT. The arrows above the ATU  $H$  component magnetogram within this time interval mark six negative  $H$  component deflections and corresponding flow events of varying amplitude, which may be related to 6 distinct optical events in the postnoon sector.

## 4. Discussion

### 4.1. Background Information on Plasma Convection With Relevance to IMF Conditions

The auroral transients considered here (1130–1230 UT) belong to an extended sequence following the onset of

activity observed above Svalbard at about 1030 UT on January 7, 1992. The characteristics of the onset itself has been reported by *Lockwood et al.* [1993a] and was accompanied by an equatorward migration of the red arc (polar cap expansion) and a major increase in plasma convection (EISCAT observations in postnoon sector). They found this onset to be consistent with a southward turning of the IMF (IMF data not available). The  $H$  component of the Greenland magnetograms reveals that a corresponding convection enhancement took place in the morning cell around 1030 UT as well (cf. Figure 7). The F11 plasma drift observations (cf. Figure 6) are consistent with such a major increase in the high-latitude plasma flow after the northern hemisphere pass at 0957 UT but prior to the southern hemisphere crossing at 1050 UT.

The high-latitude convection patterns encountered by F11 passes within the time interval from 1050 to 1230 UT (including the time of interest) were those characteristic of negative IMF  $B_y$ . The negative  $H$  component deflections in Greenland in the prenoon sector during this time interval, is in accordance with an extensive morning cell as expected for a negative IMF  $B_y$  [cf. *Heppner and Maynard*, 1987; *Freeman et al.*, 1993].

The cross-polar potential drops measured by F11 during the 1050, 1139, and 1229 UT northern and southern hemisphere passes were 70, 40, and 54 kV, respectively. As F11 here flew close to the dawn-dusk meridian, the obtained values are assumed to be reasonably good estimates of the total transpolar voltage [*Heppner and Maynard*, 1987]. The moderate values of the cross polar cap voltage indicate that

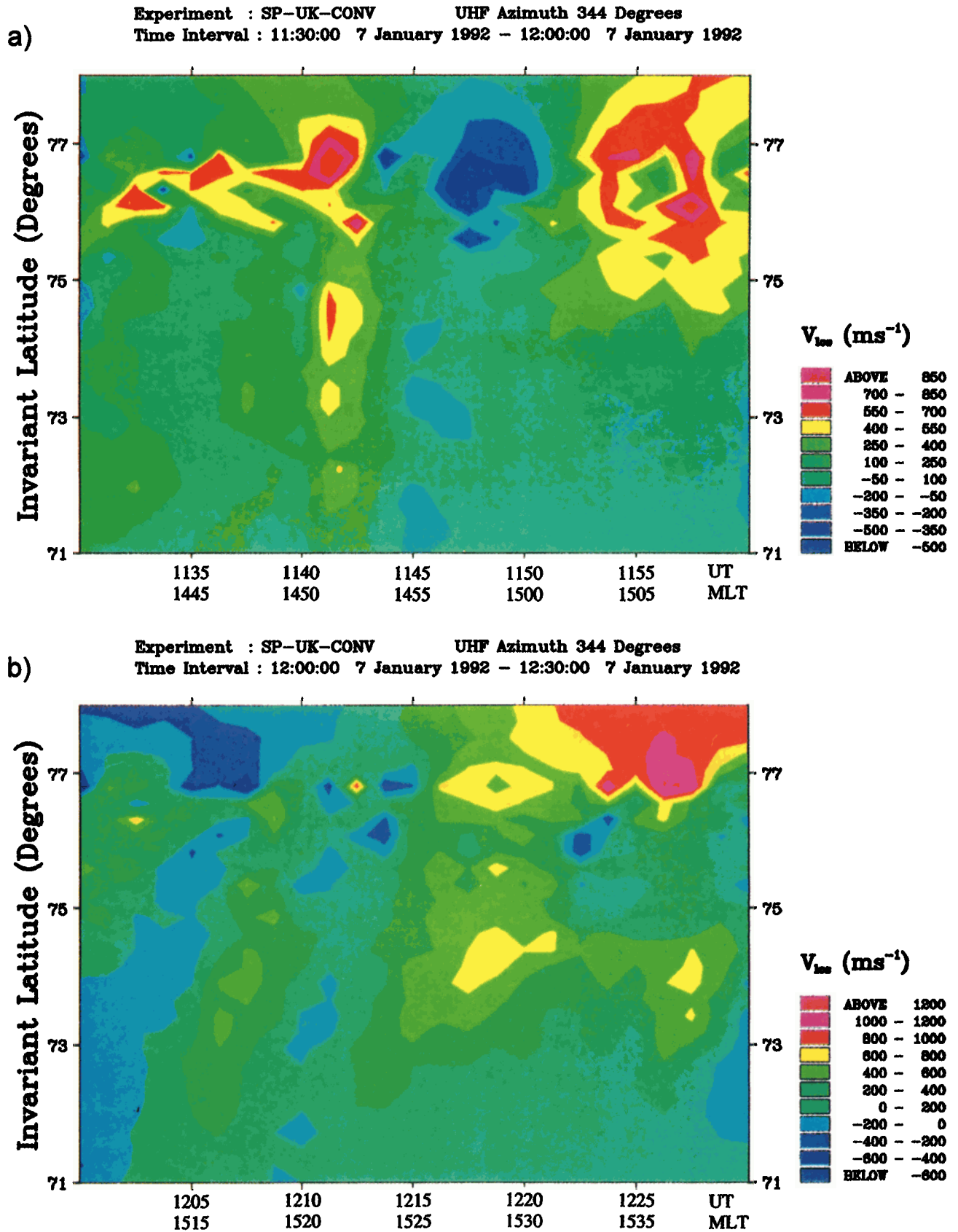
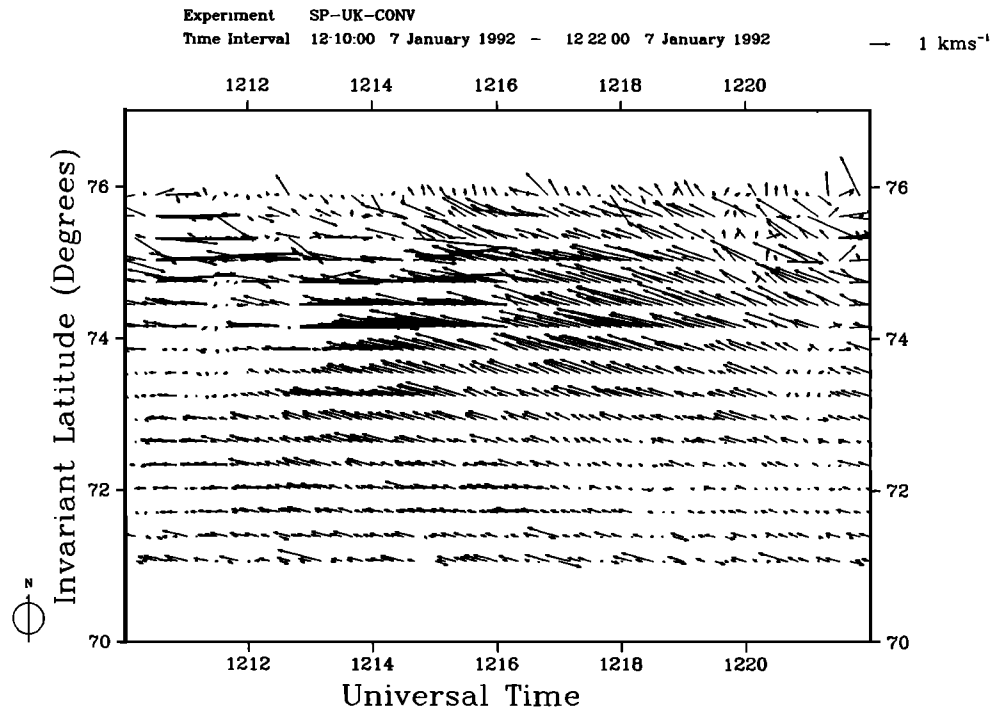


Plate 3. (a) The line-of-sight velocity measured by the EISCAT UHF radar versus time and invariant latitude during the time period 1130-1200 UT (1440-1510 MLT). Negative (positive)  $v_{los}$  corresponds to equatorward (poleward) plasma motion. (b) Same as Figure 3 for 1200-1230 UT (1510-1540 MLT).



**Figure 5.** The 10-s resolution ion drift vectors at 17 range gates, covering 71°–76° ILAT, as function of time. The flow vectors are obtained by operating the EISCAT UHF and VHF radars simultaneously in the SP-UK-CONV mode.

the IMF  $B_z$  component was small in this case [Doyle and Burke, 1983].  $K_p$  was 2<sup>+</sup> during the periods 0900–1200 and 1200–1500 UT on January 7, 1992.

#### 4.2. Convection Reversal Boundary in Relation to Auroral Forms

EISCAT flow vectors as shown in Figure 5 reveal that the direction of the ionospheric plasma flow was steadily northwest over the whole range of invariant latitudes from 71° to 76°. However, only a minor flow speed was observed at the northernmost radar gate, and the convection reversal was likely located near the Ny Ålesund latitude (76° ILAT). The northern F11 pass at 1139 UT crossed the evening convection reversal at ~75.5° ILAT (~1730 MLT). The auroral forms poleward of the background emission propagated eastward with speeds similar to the ion drift velocity observed there (cf. Figure 3 and Plate 2b). It is suggested that the flow reversal was located close to the poleward border of the background aurora, which hence was located predominantly on sunward/westward convecting field lines.

The two components of auroral activity, i.e., the background luminosity and the intermittent auroral forms immediately poleward of it, show significantly different spectral characteristics (cf. Figure 2) which indicates a transition boundary between two different sources of particle precipitation. The sequence of eastward convecting 630.0 nm auroral forms were almost absent in the green line which indicates a strong influx of soft (a few hundred eV) electrons. The luminous background aurora on the other hand, located on westward convecting flux tubes, contain a mixture of 630.0 nm and 557.7 nm emissions. Discrete events of auroral brightening at 557.7 nm indicate electron precipitation accelerated through kV field-aligned potential

drops. These active auroras were almost always present in this region (Figure 2) and, as will be considered in section 4.4, were likely associated with field-aligned currents (FACs) out of the ionosphere.

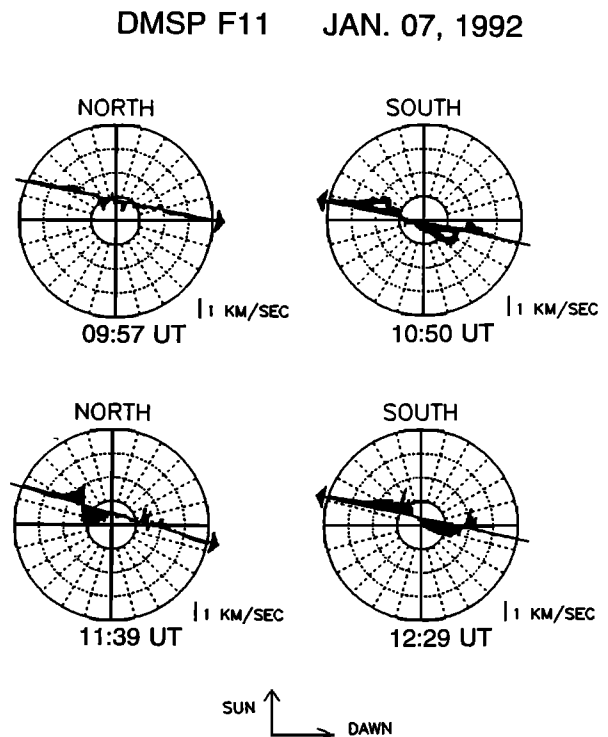


**Figure 6.** F11 cross-track component of plasma flow during four successive northern and southern hemisphere passes.

A sharp transition boundary of particle precipitation was observed by DMSP F10 at 1154.45 UT ( $\sim 76^\circ$  MLAT, 13 MLT). This precipitation boundary was roughly coincident with the convection reversal boundary. The region of hard electron precipitation detected equatorward of this boundary appears to be of central plasma sheet origin, i.e., a trapped population of high-energetic plasma drifting in from the nightside. From 1146 to 1150 UT, F10 crossed through a region of spatially and spectrally structured electron and ion precipitation, likely associated with discrete forms of the nightside oval. The spectral characteristic of this region resembles what *Newell et al.* [1991] classified as a low-altitude signature of the boundary plasma sheet (BPS). Poleward of these precipitation zones and the convection reversal, F10 traversed moving auroral forms coincident with a high flux of magnetosheath-like precipitation (cf. Figures 3 and 4; Plate 2a). Although F10 crossed through the background auroral arc outside the region of optical coverage, these observations support the view that a precipitation boundary likely existed in between the background aurora and the auroral transients, in the near vicinity of the flow reversal.

The precipitation boundary near 1154.45 UT ( $\sim 76^\circ$  MLT,  $\sim 13$  MLT; Plate 2a) has three apparent characteristics: It represents a sharp equatorward boundary of the magnetosheath-like particle precipitation. It marks a poleward boundary of the influx of energetic electrons. The background of energetic ion fluxes on the other hand, is present on either side of this boundary. According to *Lyons et al.* [1994], these are all key features of the equatorward edge of an open LLBL, at least for the near noon region as investigated by them.

This secondary ion population may also be the maximum energy tail of magnetosheath plasma injected by magnetic reconnection. When a magnetic flux tube has been opened at the magnetopause, magnetosheath plasma will cross the boundary for the entire time period it is open. For a certain time period, about 10 min, the magnetic field liberates energy to the magnetosheath particles which make them able to precipitate down into the ionosphere [*Lockwood and Smith*, 1994]. The ions are speeded up across the rotational discontinuity at the magnetopause to approximately the Alfvén speed. For this particular case, the bulk of low-energy ions might have been injected closer to the X line than the higher energy ions, encompassed in such a way that the two populations occasionally entered the ionosphere at the same time [*Lockwood*, 1995].

According to the statistical work conducted by *Newell and Meng* [1992, 1994] the southern edge of the LLBL actually border on the CPS in the early afternoon hours, whereas it later on in the afternoon border on the BPS. The convection reversal boundary usually occur within the LLBL footprint, or may coincide with the LLBL/BPS particle boundary [e.g., *Heelis et al.*, 1976; *Newell et al.*, 1991]. Whether or not the persistent cleft precipitation in this case originates from the BPS or the inner edge of the LLBL is quite uncritical for this study. What is most important to note is that the auroral transients and the background aurora are separated by the convection reversal boundary and that the particles producing the two categories of auroral activity must have been injected by different magnetospheric source mechanisms. The moving auroral forms poleward of the flow reversal are taken as a signature of the temporal/spatial behavior of

## GREENLAND

### MAGNETOMETER CHAIN

H JAN 7 1992

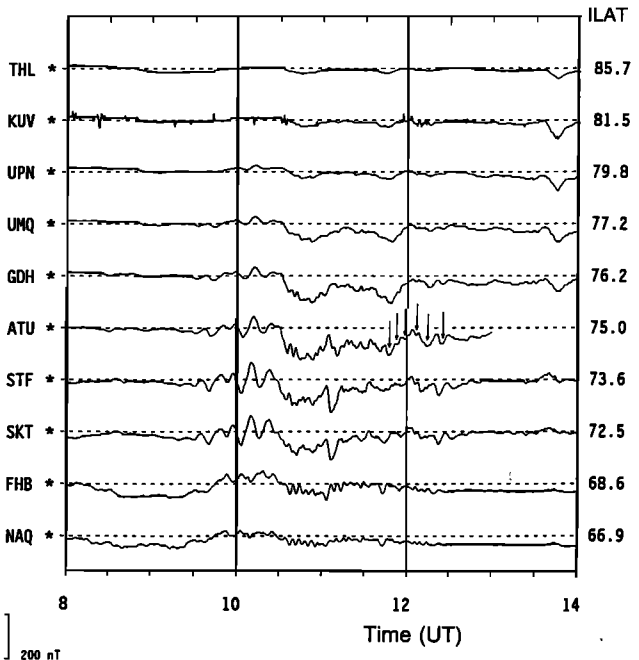


**Figure 7.** Magnetometer data ( $H$  components) from Greenland west coast ground stations for the time interval 1000-1400 UT. See text for details.

precipitation along open flux tubes. We assume that the poleward edge of the persistent aurora marks the polar cap boundary.

### 4.3. Auroral Transients and Flow Excitation

In the postnoon sector on the actual day the ionospheric plasma flow was continuously recorded by EISCAT over the range of latitudes  $71^\circ$ - $76^\circ$  ILAT. The radar field of view was located within the sunward convecting part of the evening convection cell. In order to demonstrate the temporal variations of westward/sunward flow ( $v_w$ ), the voltage ( $V$ ) across the radar field of view has been estimated from  $V = \sum_n v_w B_i dl$ , where the sum is over all the  $n=17$  gates,  $B_i$  is the local magnetic field and  $dl$  is the distance between  $L$  shells of adjacent gates ( $\sim 35$  km). Note that  $V$  is the sunward/westward flux transfer rate through the EISCAT field of view. The Greenland west coast chain of magnetometers provide qualitative information about variations of the convection in the morning cell. It should be emphasized that EISCAT and the Greenland magnetometers covered only the sunward convecting parts of the flow cells. Poleward of the convection reversal boundary we have flow information only from DMSP F10 and F11.

As discussed in section 4.1. the activity at  $\sim 1030$  UT was accompanied by enhanced convection in both the prenoon and the postnoon ionosphere. This observation supports the conclusion drawn by *Lockwood et al.* [1993a] that this activity onset was accompanied by generation of large-scale convection. They interpreted their observations according to the *Cowley and Lockwood* [1992] model of flow excitation due to pulsed magnetic reconnection. Here we will focus on

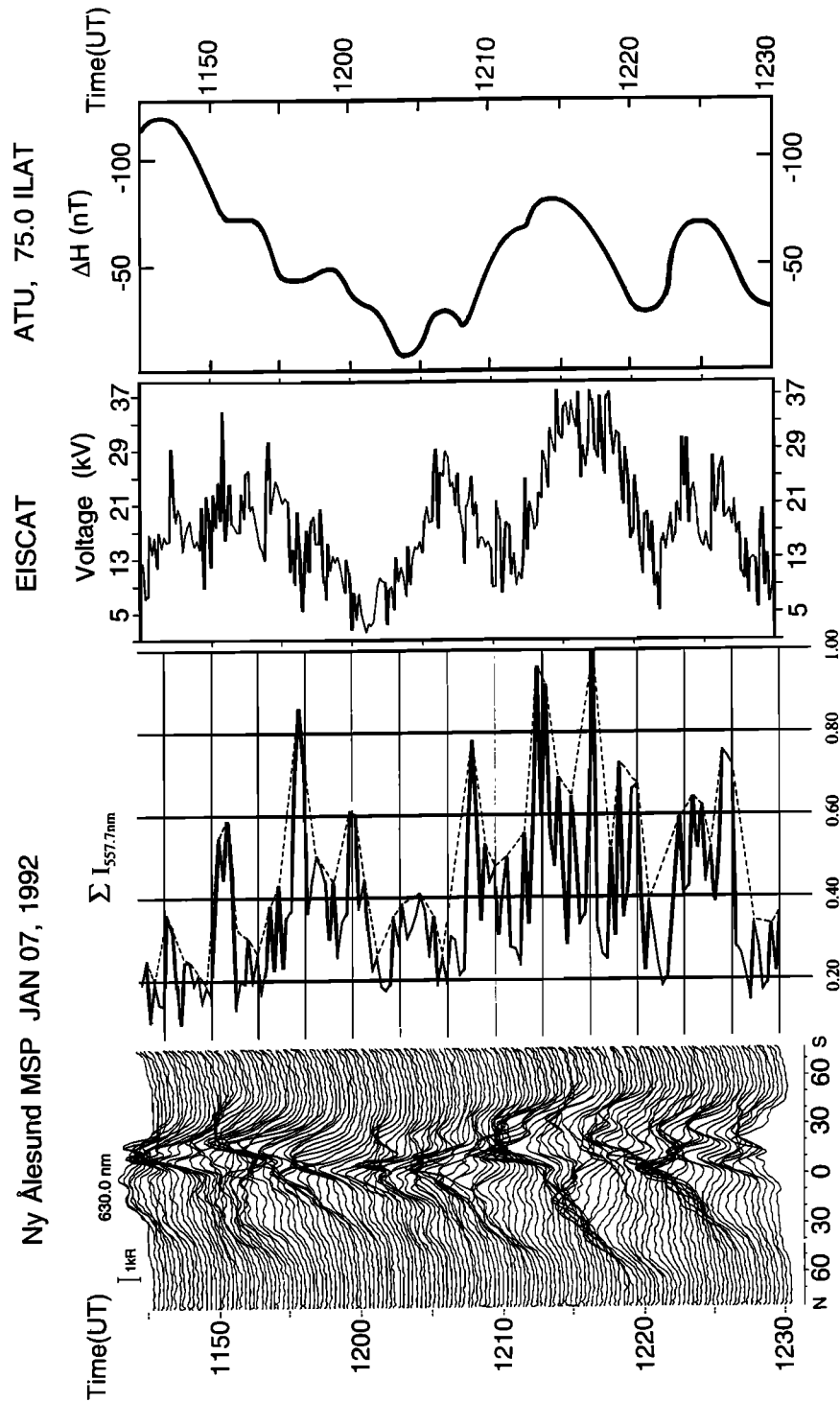


**Figure 8.** Detailed multipoint observations for the period 1145-1230 UT. The four panels include from left: Photometer scans, showing 630.0 nm intensity as a function of zenith angle; the normalized value of the 557.7 nm intensity integrated over each north-south MSP scan; EISCAT flow voltage data associated with westward flow; the  $H$  component magnetometer deflection from station ATU (75°ILAT) at West Greenland. The integrated 557.7 nm intensity in the second panel is thought to be an indicator of the postnoon region 1 current. Enhanced  $H$ -component deflections in the right panel provide qualitative information about the variability of the sunward convection above Greenland.

temporal variations of high-latitude convection associated with a regular sequence of optical events. For this purpose we have selected the time interval 1145–1230 UT.

The four panels in Figure 8 include from the left: stacked photometer traces at wavelength 630.0 nm, the normalized value of the 557.7 nm intensity integrated over each north-south MSP scan versus time, EISCAT flow voltage, and the  $H$  component magnetometer data from ATU (75° ILAT) on the west coast of Greenland. In the left panel a sequence of six auroral transients were monitored poleward of the background cleft auroral activity during the time interval from 1145 to 1230 UT. The flow voltage in panel 3 refers to the adjacent region immediately equatorward of the eastward moving transients. It is noticeable that the flow excitation associated with the first three events (5-min repetition period) were smoothed together in basically one flow enhancement peaking at ~20 kV. The convection decayed to zero between events 3 and 4 (12 min apart). Furthermore the convection voltage associated with the last three events at 1210, 1218, and 1226 UT (8 min apart) were apparently correlated with the auroral transients although the convection did not decay to zero between successive bursts. The  $H$  component magnetometer data from ATU (75° ILAT) refer to the station above which the southwestward directed Hall current was centered. We recall that enhanced negative deflection is consistent with enhanced sunward convection within the morning cell. As in the afternoon sector the first three events seem to merge into one major flow-enhancement. The first very pronounced flow minimum observed by EISCAT at 1201 UT took place about 3 min before a corresponding minimum in Greenland deflections. The last three postnoon and prenoon flow bursts were practically in phase, which strongly indicate that the auroral activity was accompanied by enhanced ionospheric return flow on either side of noon.

When interpreting local flow measurements, such as the EISCAT data here, one must be aware of the untrivial problem of distinguishing between local distortions of the large-scale flow pattern and/or time variability of large-scale convection. Let us first consider the possibility that the burst-like flow enhancements observed by EISCAT were the return flow set up equatorward of a train of FTE/PTE magnetic flux ropes being pulled through the ionosphere from west to east. According to a "moving cloud" model, each of the transient auroral forms is to be attributed to the cross section of the individual flux ropes. Hence EISCAT could be sampling only the westward return flow set up equatorward of the flux tubes. In this geometry, EISCAT could be viewing at most one quarter of successive double vortex flow patterns passing by. As the flow bursts were located within the latitude interval from 72.5° to 75.5° ILAT, a scale size of ~1300 km is estimated for a double vortex system. The east-west extension of a flow pattern moving across the radar beams equals the time it took it to pass times the travelling speed of the event. In this case, since the background flow was minor, the travelling speed of the flux rope is likely to be of the same order as the return flow speed. A typical flow burst with a speed of 2.5 km s<sup>-1</sup> lasting about 8 min, is consistent with an east-west extent of 1200 km. If the flow bursts actually were related to flow vortices passing through the radar field of view in the way suggested above, one would expect that the direction of flow was changing. In particular, equatorward flow should be

observed at the leading edge of the event and this would rotate to poleward, via westward as the vortex passed by. As seen from Figure 5 this was indeed not the case. The north-south component of the vectors shown is directly measured by the UHF radar (which was pointing approximately along the magnetic meridian), and it can be seen that southward flow is absent from the onset of the flow burst starting at 1213 UT. Instead the  $v_{los}$  was coincident with the north-south motions of the background arc (cf. section 3.3). Thus we exclude the possibility of localized twin-vortical convection vortices of the FTE/PTE type discussed by *Southwood* [1987], *Wei and Lee* [1990], *Lockwood et al.* [1990b] and *Newell and Sibeck* [1993]. By using similar arguments we, exclude the presence of traveling twin vortices generated by Kelvin-Helmholtz instability and/or pressure pulses.

It is widely accepted that the northern-southern hemisphere dawn-dusk asymmetry of flow patterns is a reconnection related phenomenon controlled by the  $B_y$  component of the IMF [*Heppner and Maynard*, 1987]. According to existing models of the open magnetosphere [*Jørgensen et al.*, 1972; *Cowley*, 1981] IMF  $B_y$  related magnetic field stresses give rise to an initial east-west motion of newly reconnected flux tubes in opposite direction at the two hemispheres. This is believed to be a most appropriate manifestation of the open magnetosphere. The variations of a type DE convection pattern may be explained by the *Cowley and Lockwood* [1992] model of flow excitation in response to pulsed magnetic reconnection (cf. Introduction). The basic principle of this model is that flux may be added to or removed from the polar cap only in the regions which map to the dayside and nightside neutral lines, respectively. No flux crosses the polar cap boundary anywhere else, which means that the polar cap boundary moves radially with the same speed as the plasma flow. In particular, polar cap boundary motions, as a consequence of unbalanced dayside or nightside reconnection, generate the commonly observed two-cell pattern of high-latitude convection [see *Lockwood et al.*, 1990a, 1993a].

In section 3.3, we found that north-south motions of the equatorward boundary of the background aurora was consistent with corresponding line-of-sight velocities observed by the UHF radar. At higher latitudes, the radar measured line-of-sight velocities that were considerably higher. We recall that the antenna was pointing approximately along the magnetic meridian. However, if the convection streamlines happened to make an angle with the  $L$  shell of a few degrees, the events of enhanced zonal flow could make a considerable contribution to the north-south motions as observed by EISCAT. Faster moving plasma at higher latitudes occurred in periods of enhanced flow and concurrent poleward motion of the background arc. The fact that plasma to be associated with open flux (poleward of ~76°) moved equatorward during intervals of polar cap expansion (magnetospheric erosion) exclude the possibility of an expanded reconnection line in the ~15–16 MLT sector. Furthermore, if the reconnection line actually extended into the optical field of view, the moving auroral forms should have emerged out of the background cusp aurora (cf. Introduction).

During the time interval from 1145 to 1230 UT, the polar cap expanded twice, both times being associated with peak levels of the EISCAT flow voltage. According to *Cowley and Lockwood* [1992], it takes ~15 min to reestablish a new

equilibrium after a transient addition of open flux to the polar cap during which the polar cap has expanded. The average period of polar cap boundary motions observed here was of the same order as this ionospheric response time. When the event repetition time is less than the equilibrium time constant, more than one event drives flow at any one time [Smith *et al.*, 1992]. Thus the first three events in Figure 8, 5 min apart, gave rise to continuous flow within 1145–1200 UT. As the event period increased, flow variations related to the individual events became more prominent (event 4, 5, and 6 with eight min recurrence period) as expected.

The EISCAT flow voltage which is representative for the voltage across the evening convection cell was observed to vary between 2 and 35 kV in response to the auroral activity. Hence the background convection during the actual period was negligible. The EISCAT flow voltage was ~20 kV on average. This is about 50% of the transpolar voltage derived by F11 during the northern hemisphere pass at 1139 UT (section 3.4). The amplitude of the transauroral voltage exceeds that seen during northward IMF and hence is unlikely to have a viscous-like origin. We therefore conclude that the temporal fluctuations of the polar cap convection was controlled by time-varying reconnection at the dayside magnetopause. The data do, however, not allow us to say how time-varying.

#### 4.4 Variability of Flow Voltage and 557.7 nm Emission Intensity

The strong 557.7 nm auroral brightenings displayed within the postnoon background aurora (see Figure 2) are consistent with level enhancements of upward region 1 current expected to occur in this local time sector [Iijima and Potemra, 1978]. Enhanced green line intensity indicates precipitating electrons being accelerated through a field-aligned potential drop. As a first order of approximation, these electrons can be treated as a beam of monoenergetic electrons. In the case of monoenergetic electron precipitation, the auroral emission intensity is expected to be proportional to the electron number flux and hence the current density. Panel 2 (from left) in Figure 8 shows the normalized value of the 557.7 nm intensity integrated over each north-south MSP scan versus time for the period 1145–1230 UT. (An integrated representation of the 557.7 nm intensity is chosen since the latitude position of the peak intensity exhibited a rapid temporal variation, see Figure 2.) In order to emphasize the 557.7 nm peak intensity variations a dashed curve connecting all the maximum points has been drawn. (The minima points of this curve does not necessarily mean that the auroral activity was low but rather that the photometer in the scanning mode failed to detect the auroral activity at any one time.) This "maximum curve" of green-line intensity follows systematically the variations of the EISCAT flow voltage. Source of variability of the "maximum" 557.7 nm curve may partly be due to the effect of time-varying field-aligned potential drop. An additional contribution is the changing zenith angle position of the arc brightenings. The relatively good correlation between 557.7 nm intensity variations and convection voltage suggests a close relation between the flow voltage and the upward field-aligned current intensity. Enhanced convection electric fields in the ionosphere (driven by magnetospheric convec-

tion) are accompanied by enhanced Birkeland current as expected.

#### 4.5. Moving Auroral Forms and Related Boundary Layer Phenomena

A close correlation between a sequence of auroral forms and large-scale convection enhancements has been documented. We have concluded that the ionospheric convection was likely to be driven by magnetic reconnection. The possibility that the moving auroral forms signify a viscous process is not totally excluded, however.

Phenomenologically, by means of motion pattern, spectral characteristics, spatial scale size and recurrence frequency, the moving auroral forms bear strong resemblance to the specific category of events reported by Sandholt *et al.* [1986, 1989, 1993a, b]. The initial east-west motion around noon of this class of events is controlled by the IMF  $B_y$  polarity, a property which relates this category of events to pulsed reconnection at the dayside magnetopause. Specifically, during IMF  $B_y$  negative conditions, magnetic tension will pull an open flux tube formed in the noon/late prenoon sector eastward into the postnoon sector [Cowley *et al.*, 1991]. For  $F$  layer emissions the all-sky TV camera has a local time coverage of maximum 3 hours, i.e., at 1150 UT (~15 MLT) the field of view spanned roughly the 1330 to 1630 MLT sector. The auroral forms which moved into the all-sky camera field of view from west must have been formed closer to magnetic noon; we cannot say exactly where. The ion dispersion signature observed by F10 in the near noon et region (Plate 2a) may be attributed to the reconnection related "velocity filter" effect [e.g. Newell *et al.*, 1988; Cowley *et al.*, 1991; Onsager *et al.*, 1993]. The highest-energy ions, corresponding to the most recently reconnected field lines, were found at the equatorward edge of the event (Plate 2a). Thus, the sequence of auroral events is a candidate footprint signature of FTE remnants.

The motion of a newly reconnected flux is generally controlled by magnetic tension and solar wind/magnetosheath flow (cf. Introduction and references therein). However, these forces change along the magnetopause, i.e., the net force acting on the open flux is inhomogeneous. This may explain the observation that the longitudinal extended auroral forms tend to rotate (cf. Plate 1) while the smaller arc fragments do not. However, as noted in section 3.1, the vorticity may not be real.

Despite the overall support our observations give to time varying reconnection some problems remain. It is quite critical for this case study that we are not able to determine with certainty whether the moving auroral forms were located on open or closed magnetic field lines. Hence the possibility that the auroral forms were caused by a viscous mechanism cannot be definitely excluded. The sequence of auroral forms continued until the end of observations that day about 1330 UT (16.6 MLT). It is questionable if magnetosheath plasma can encounter the ionosphere through a flux tube with its footprint at ~16 MLT. Reconnection at the dusk flank is rather unlikely for the negative IMF  $B_y$  conditions inferred from the F11 polar cap convection data.

Another candidate boundary layer mechanism is impulsive magnetosheath plasma injections onto closed field lines. The ionospheric signature of such a plasma transfer event (PTE) across the frontside magnetopause is expected to propagate

equatorward across the convection reversal and cleft arc with a subsequent tailward motion [cf. Heikkila, 1989; Lundin and Evans, 1985; Goertz *et al.*, 1985]. Woch and Lundin [1992] reported on a class of plasma penetration events which predominate around 16 MLT. The filamentary blobs of magnetosheath plasma were identified by them within the region populated by ring current/plasma sheet particles, deep inside the region of sunward convection. In contrast, the events considered here propagated along the flow reversal boundary on the poleward side of the cleft aurora. The auroral forms were not moving equatorward relative to the cleft arc as expected for plasma blobs injected into the LLBL. Plasma injections directly into the mantle region by a similar mechanism as in the LLBL may provide another possibility. However, according to the standard boundary layer dynamo model proposed for plasma transfer events, injected plasma filaments are getting polarized as electrons and ions diverge under the action of the Lorentz force, and the magnetosheath plasma characteristics are expected to be blurred out. Such plasma clouds are depolarized via a pair of Birkeland currents which close in the conducting ionosphere (load). Discrete auroras are expected to be associated with the upward field-aligned current sheet connected to the negatively charged edge of the injected plasma cloud. By such arguments discrete arcs commonly observed in the postnoon sector have tentatively been attributed to the plasma penetration process [Meng and Lundin, 1986].

Sibeck [1990] proposed that quasi-periodic solar wind/magnetosheath pressure pulses may trigger auroral events which are similar to FTE signatures. A chain of pressure pulses impinging the frontside magnetopause may also modulate the reconnection rate [Scurry and Russell, 1991]. Therefore the enhanced convection events and the auroral transients may be triggered at the same time by solar wind pressure pulses, but without a causal relation between the two features.

## 5. Summary and Concluding Remarks

Eastward moving auroral forms observed in the postnoon sector has been related to events of enhanced convection on either side of noon. A cartoon sketch shown in Figure 9 summarizes the observations. A series of 630.0 nm auroral transient forms, formed outside the optical field of view (marked by the circle), propagated eastward on the poleward side of discrete background aurora into the all-sky camera field of view within which they faded. The DMSP F10 Svalbard crossing at 1152 UT, traversing one of the moving auroral forms, is indicated by the straight line drawn through the all-sky camera field of view. The background cleft aurora (LLBL and/or BPS plasma) was located predominantly on sunward convecting field lines. The 557.7 nm emission indicates that the region 1 current was distributed within the background aurora, and the inferred current intensity varied with the flow enhancements and the 630.0 nm transients. The polar cap expanded during periods of enhanced auroral activity and convection enhancements.

The enhanced convection events were found to be consistent with a time-varying magnetic reconnection rate and corresponding modulations of Dungey cell convection. The auroral forms coincided with magnetosheath-like

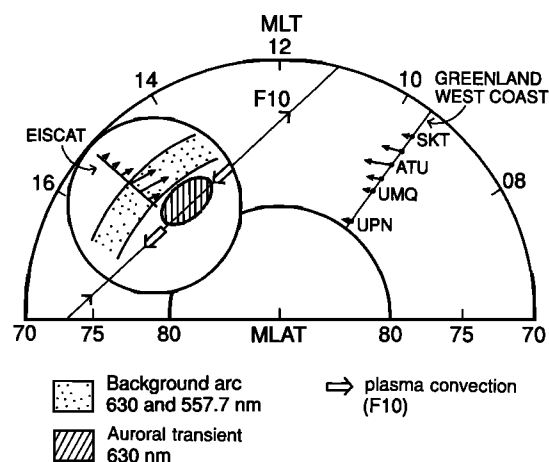


**Figure 9.** Schematic illustration summarizing the observations. See text for explanation.

particle precipitation and they moved eastward with a speed comparable with the local convection velocity. A secondary population of energetic ions, however, introduced an uncertainty whether or not the moving auroral forms themselves were associated with open flux tubes and hence directly related to magnetopause reconnection and the bursty ionospheric ion flow events.

Although it is well accepted that the addition of open magnetic flux contributes to the polar cap convection, the relative importance of steady state and transient reconnection is a matter of controversy [Lockwood *et al.*, 1990a; Denig *et al.*, 1993; Lockwood and Cowley, 1994]. Since the background convection was small on the actual day ( $K_p=2^+$ ), this case study supports the view that time-varying reconnection may at times be a source of major oscillations of the transpolar voltage.

**Acknowledgments.** It is a great pleasure to thank the director and the staff of the EISCAT Scientific Association for their assistance. EISCAT is supported by the research councils of the six member nations: France, Germany, UK, Sweden, Finland, and Norway. Optical observation campaigns in Ny Ålesund have strongly benefitted from economical and technical support from the Norwegian Polar Research Institute. The work was partly completed during the J. Moen's Window on Science trip (WOS-92-2102) to the Phillips Laboratory/ Geophysics Directorate sponsored by the US Air Force Office of Scientific Research and visit to Rutherford Appleton Laboratory founded by NAVF and the British Council. This project has also been given financial support from "Nansenfondet og de dermed forbundne fond" (grant 154/92).

The Editor thanks N. C. Maynard and R. A. Greenwald for their assistance in evaluating this paper.

## References

- Cowley, S. W. H., Magnetospheric asymmetries associated with Y-component of the IMF, *Planet. Space. Sci.*, 29, 76-79, 1981.
- Cowley, S. W. H., The causes of convection in the earth's magnetosphere: A review of developments during the IMS, *Rev. Geophys.*, 20, 531-565, 1982.
- Cowley, S. W. H., M. P. Freeman, M. Lockwood, and M. F. Smith, The ionospheric signatures of flux transfer events, in *Cluster Dayside Polar Cusp*, Eur. Space Agency Spec. Publ., ESA SP-330, 105-112, 1991.

- Cowley, S. W. H., and M. Lockwood, Excitation and decay of solar wind-driven flows in the magnetosphere-ionosphere system, *Ann. Geophys.*, **10**, 103-115, 1992.
- Denig, W. F., W. J. Burke, N. C. Maynard, F. J. Rich, B. Jacobsen, P. E. Sandholt, A. Egeland, S. Leontjev, and V. G. Vorobjev, Ionospheric signatures of dayside magnetopause transients: A case study using satellite and ground measurements, *J. Geophys. Res.*, **98**, 5969-5980, 1993.
- Doyle, M. A., and W. J. Burke, S3-2 measurements of the polar cap potential, *J. Geophys. Res.*, **88**, 9125-9133, 1983.
- Etemadi, A., S. W. H. Cowley, M. Lockwood, B. J. I. Bromage, D. M. Willis, and H. Lühr, The dependence of high-latitude dayside ionospheric flows on the north-south component of the IMF: A high time resolution correlation analysis using EISCAT "Polar" and AMPTE UKS and IIRM data, *Planet. Space Sci.*, **36**, 471-498, 1988.
- Freeman, M. P., and D. J. Southwood, The effect of magnetospheric erosion on mid- and high-latitude ionospheric flows, *Planet. Space Sci.*, **36**, 509-522, 1988.
- Freeman, M. P., C. J. Farrugia, L. F. Burlaga, M. R. Hairston, M. E. Greenspan, J. M. Ruohoniemi, and R. P. Lepping, The interaction of a magnetic cloud with the Earth: Ionospheric convection in the northern and southern hemispheres for a wide range of quasi-steady interplanetary magnetic field conditions, *J. Geophys. Res.*, **98**, 7633-7655, 1993.
- Friis-Christensen, E., M. A. McHenry, C. R. Clauer, and S. Vennestrom, Ionospheric travelling convection vortices observed near the polar cleft: A triggered response to sudden changes in the solar wind, *Geophys. Res. Lett.*, **15**, 253-256, 1988.
- Glassmeier, K.-H., Travelling magnetospheric convection twin-vortices: observation and theory, *Ann. Geophysicae.*, **10**, 547-565, 1992.
- Goertz, C. K., E. Nilsen, A. Korth, K. H. Glassmeier, C. Haldoupis, P. Hoeg, and D. Hayward, Observations of possible ground signatures of flux transfer events, *J. Geophys. Res.*, **90**, 4069-4078, 1985.
- Heelis, R. A., W. B. Hanson, and J. L. Burch, Ion convection velocity reversals in the dayside cleft, *J. Geophys. Res.*, **81**, 3803-3809, 1976.
- Heikkila, W. J., T. Stockflet Jörgensen, L. J. Lanzerotti, and C. G. MacLennan, A transient auroral event on the dayside, *J. Geophys. Res.*, **94**, 15291-15305, 1989.
- Heppner, J. P., and N. C. Maynard, Empirical high-latitude electric field models, *J. Geophys. Res.*, **92**, 4467-4490, 1987.
- Iijima, T., and T. A. Potemra, Large-scale characteristics of field aligned currents associated with substorms, *J. Geophys. Res.*, **83**, 599-615, 1978.
- Jørgensen T. S., E. Friis-Christensen, and J. Wilhelm, Interplanetary magnetic-field direction and high-latitude ionospheric currents, *J. Geophys. Res.*, **77**, 1976-1977, 1972.
- Kivelson, M. G., and D. J. Southwood, Ionospheric travelling vortex generation by solar wind buffeting of the magnetosphere, *J. Geophys. Res.*, **96**, 1661-1667, 1990.
- Lockwood, M., Overlapping cusp ion injections: An explanation invoking magnetopause reconnection, *Geophys. Res. Lett.*, **22**, 1141-1144, 1995.
- Lockwood, M., and S. W. H. Cowley, Comment on "ionospheric signatures of daytime magnetopause transients: A case study using satellite and ground measurements" by Denig et al., *J. Geophys. Res.*, **99**, 4253-4255, 1994.
- Lockwood, M., and M. P. Freeman, Recent ionospheric observations relating to solar wind-magnetosphere coupling, *Philos. Trans. R. Soc. London., Ser. A*, **328**, 93-105, 1989.
- Lockwood, M., and M. F. Smith, Low and middle altitude cusp particle signatures for general magnetopause reconnection rate variations, 1, Theory, *J. Geophys. Res.*, **99**, 8531-8553, 1994.
- Lockwood, M., P. E. Sandholt, S. W. H. Cowley, and T. Oguti, Inter-planetary magnetic field control of dayside auroral activity and the transfer of momentum across the dayside magnetopause, *Planet. Space Sci.*, **37**, 1347-1365, 1989.
- Lockwood, M., S. W. H. Cowley, and M. P. Freeman, The excitation of plasma convection in the high-latitude ionosphere, *J. Geophys. Res.*, **95**, 7961-7972, 1990a.
- Lockwood, M., P. E. Sandholt, A. D. Farmer, S. W. H. Cowley, B. Lybekk, and V. N. Davda, Auroral and plasma flow transients at magnetic noon, *Planet. Space Sci.*, **38**, 973-993, 1990b.
- Lockwood, M., J. Moen, S. W. H. Cowley, A. D. Farmer, U. P. Løvhaug, H. Lühr, and V. N. Davda, Variability of dayside convection and motions of the cusp/cleft aurora, *Geophys. Res. Lett.*, **20**, 1011-1014, 1993a.
- Lockwood, M., W. F. Denig, A. D. Farmer, V. N. Davda, S. W. H. Cowley, and H. Lühr, Ionospheric signatures of pulsed reconnection at the Earth's magnetopause, *Nature*, **361**, 424-427, 1993b.
- Lundin, R., and D. S. Evans, Boundary layer plasmas as a source for high-latitude, early afternoon, auroral arcs, *Planet. Space Sci.*, **33**, 1389-1406, 1985.
- Lyons, L. R., M. Schulz, D. C. Pridmore-Brown, and J. L. Roeder, Low-latitude boundary layer near noon: An open field line model, *J. Geophys. Res.*, **99**, 17,367-17,377, 1994.
- McHenry, M. A., C. R. Clauer, E. Friis-Christensen, P. T. Newell, and J. D. Kelly, Ground observations of magnetospheric boundary layer phenomena, *J. Geophys. Res.*, **95**, 14,995-15,005, 1990a.
- McHenry, M. A., C. R. Clauer, and E. Friis-Christensen, Relationship of solar wind parameters to continuous, dayside, high latitude travelling ionospheric vortices, *J. Geophys. Res.*, **95**, 15,007-15,022, 1990b.
- Meng, C.-I., and R. Lundin, Auroral morphology of the midday oval, *J. Geophys. Res.*, **91**, 1572-1584, 1986.
- Newell, P. T., and C.-I. Meng, The cusp and the cleft/boundary layer: low-altitude identification and statistical local time variation, *J. Geophys. Res.*, **93**, 14,549-14,556, 1988.
- Newell P. T., and C.-I. Meng, Mapping the dayside ionosphere to the magnetosphere according to particle precipitation characteristics, *Geophys. Res. Lett.*, **19**, 609-612, 1992.
- Newell, P. T., and C.-I. Meng, Ionospheric projections of magnetospheric regions under low and high solar wind pressure conditions, *J. Geophys. Res.*, **99**, 273-286, 1994.
- Newell, P. T., and D. G. Sibeck,  $B_y$  fluctuations in the magnetosheath and azimuthal flow velocity transients in the dayside ionosphere, *Geophys. Res. Lett.*, **20**, 1719-1722, 1993.
- Newell, P. T., W. J. Burke, E. R. Sanchez, C.-I. Meng, M. E. Greenspan, and C. R. Clauer, The low-latitude boundary layer and the boundary plasma sheet at low altitude: Dayside precipitation regions and convection reversal boundaries, *J. Geophys. Res.*, **96**, 21,013-21,023, 1991.
- Onsager, T. G., C. A. Kletzing, J. B. Austin, and MacKiernan, Model of magnetosheath plasma in the magnetosphere: Cusp and mantle particles at low-altitudes, *Geophys. Res. Lett.*, **20**, 479-482, 1993.
- Pinnock, M., A. S. Rodger, J. R. Dudeney, K. B. Baker, P. T. Newell, R. A. Greenwald, and M. E. Greenspan, Observations of an enhanced convection channel in the cusp ionosphere, *J. Geophys. Res.*, **98**, 3767-3776, 1993.
- Reiff, P. H., and J. L. Burch, IMF  $B_y$ -dependent plasma flow and Birkeland currents in the dayside magnetosphere, 2, A global model for northward and southward IMF, *J. Geophys. Res.*, **90**, 1595-1609, 1985.
- Rich, F. J., and M. Hairston, Large-scale convection patterns observed by DMSP, *J. Geophys. Res.*, **99**, 3827-3844, 1994.
- Russell, C. T., and R. C. Elphic, ISEE observations of flux transfer events at the dayside magnetopause, *Geophys. Res. Lett.*, **6**, 33-36, 1979.
- Sandholt, P. E., C. S. Deehr, A. Egeland, B. Lybekk, R. Viereck and G. J. Romick, Signatures in the dayside aurora of plasma transfer from the magnetosheath, *J. Geophys. Res.*, **91**, 10,063-10,079, 1986.
- Sandholt, P. E., B. Lybekk, A. Egeland, R. Nakamura, and T. Oguti, Midday auroral breakup, *J. Geomagn. Geoelectr.*, **41**, 371-387, 1989.
- Sandholt, P. E., J. Moen, D. Opsvik, W. F. Denig, W. J. Burke, Auroral event sequence at the dayside polar cap boundary: Signature of time-varying solar wind-magnetosphere-ionosphere coupling, *Adv. Space Res.*, **13**, 7-15, 1993a.
- Sandholt, P. E., J. Moen, A. Rudland, D. Opsvik, W. F. Denig, and T. Hansen, Auroral event sequences at the dayside polar cap

- boundary for positive and negative IMF  $B_y$ , *J. Geophys. Res.*, **98**, 7737-7755, 1993b.
- Scurry, L., and C. T. Russell, Proxy studies of energy transfer to the magnetosphere, *J. Geophys. Res.*, **96**, 9541-9548, 1991.
- Sibeck, D. G., A model for transient magnetospheric response to sudden solar wind dynamic pressure variations, *J. Geophys. Res.*, **95**, 3755-3771, 1990.
- Siscoe, G. L., and T. S. Huang, Polar cap inflation and deflation, *Geophys. Res. Lett.*, **90**, 543-547, 1985.
- Siscoe, G. L., W. Lotko, and B. U. Ö. Sonnerup, A high-latitude, low-latitude boundary layer model of the convection current system, *J. Geophys. Res.*, **96**, 3487-3495, 1991.
- Smith, M. F., M. Lockwood, and S. W. H. Cowley, The statistical cusp: A flux transfer event model, *Planet. Space Sci.*, **40**, 1251-1268, 1992.
- Southwood, D. J., The ionospheric signature of flux transfer events, *J. Geophys. Res.*, **92**, 3207-3213, 1987.
- Todd, H., S. W. H. Cowley, M. Lockwood, D. M. Willis and H. Lühr, Response time of high-latitude dayside ionosphere to sudden changes in the north-south component of the IMF, *Planet. Space Sci.*, **36**, 1415-1428, 1988.
- Wei, C. Q., and L. C. Lee, Ground magnetic signatures of moving elongated plasma clouds, *J. Geophys. Res.*, **95**, 2405-2418, 1990.
- Woch, J., and R. Lundin, Signatures of transient boundary layer processes observed with Viking, *J. Geophys. Res.*, **97**, 1431-1447, 1992.
- W. F. Denig, Geophysics Directorate, PL/GPSG, Hanscom Air Force Base, MA 01731.
- A. Egeland, B. Lybekk, D. Opsvik, and P. E. Sandholt, Department of Physics, University of Oslo, P. O. Box 1048 Blindern, N-0316 Oslo, Norway.
- E. Friis-Christensen, Division of Geophysics, Danish Meteorological Institute, Lyngbyvej 100, DK-2100 Copenhagen, Denmark.
- M. Lockwood, Rutherford Appleton Laboratory, Chilton, Didcot, OX11 0QX, England.
- U. P. Løvhaug, EISCAT Scientific Association, Ramfjordmoen, N-9027 Ramfjordbotn, Norway.
- J. Moen, University Courses on Svalbard, P. O. Box 156, N-9170 Longyearbyen, Norway.

(Received December 13, 1994; revised August 21, 1995; accepted August 23, 1995.)